Maximum-Correntropy-Based Kalman Filtering for Time-Varying Systems with Randomly Occurring Uncertainties: An Event-Triggered Approach

Tingli Su, Zidong Wang, *Fellow, IEEE*, Lei Zou and Fuad E. Alsaadi

Abstract

In this paper, the maximum-correntropy-based Kalman filtering problem is investigated for a class of linear time-varying systems in the presence of non-Gaussian noises and randomly occurring uncertainties. The random nature of the parameter uncertainties is characterized by a stochastic variable conforming to the Bernoulli distribution. In order to avoid unnecessary data transmission and reduce consumption of limited communication resource, the event-triggered mechanism is introduced in the sensor-to-filter channel to decide whether the data should be transmitted or not. A novel performance index is first proposed to reflect the joint effects from the non-Gaussian noises, the event-triggered mechanism as well as the randomly occurring uncertainties. Under the proposed performance index, an event-based Kalman filter is then constructed whose gain is calculated based on the maximum correntropy criterion. Finally, the effectiveness of the proposed filtering scheme is verified via a practical target tracking example.

Index Terms

Kalman filter, maximum correntropy criterion, non-Gaussian noise, event-triggered mechanism, randomly occurring uncertainties.

I. Introduction

As one of the fundamental issues in system control and signal processing, the state estimation problem has received considerable research attention over the past decades [6], [8], [17], [18], [25], [34], and a variety of state estimation schemes have been developed based on different performance indices [19], [26], [28]. Among different kinds of state estimation schemes, the well-known Kalman filtering (KF) algorithm has been deemed to be a powerful means to estimate the state of linear systems with Gaussian noises. To be more specific, the KF algorithm is, in essence, a least mean-square linear filtering scheme that aims to

The Deanship of Scientific Research (DSR) at King Abdulaziz University, Jeddah, Saudi Arabia funded this project, under grant no. (FP-22-42). This work was also supported in part by the National Natural Science Foundation of China under Grants 61903009, 61873148, 61933007 and 61703245, the Postdoctoral Special Innovation Foundation of of Shandong province of China under Grant 201701015, the Royal Society of the UK, and the Alexander von Humboldt Foundation of Germany. (*Corresponding author: Zidong Wang*)

T. Su is with the School of Artificial Intelligence, Beijing Technology and Business University, Beijing 100048, China.

Z. Wang is with the College of Electrical Engineering and Automation, Shandong University of Science and Technology, Qingdao 266590, China. He is also with the Department of Computer Science, Brunel University London, Uxbridge, Middlesex, UB8 3PH, United Kingdom. (Email: Zidong.Wang@brunel.ac.uk).

L. Zou is with the Department of Computer Science, Brunel University London, Uxbridge, Middlesex, UB8 3PH, United Kingdom.

F. E. Alsaadi is with the Department of Electrical and Computer Engineering, Faculty of Engineering, King Abdulaziz University, Jeddah 21589, Saudi Arabia.

achieve the optimal estimation by minimizing the estimation error covariance in a recursive manner. So far, the KF problems have attracted a large amount of research attention from both academia and industry with successful applications to various fields such as target tracking, fault diagnosis, econometrics, inertial navigation system, and so on [16]. Furthermore, the traditional KF algorithm has been modified to suit nonlinear systems and a number of KF variants have been available in the literature, see e.g. extended Kalman filtering [26], unscented Kalman filtering [44], and cubature Kalman filtering algorithms [1].

An implicit assumption with traditional KF algorithm (and its variants) is that the process/measurement noises are Gaussian-type. Such an assumption is, however, often too strict for real scenarios and therefore inevitably limits the application scope since *non-Gaussian* noises (e.g. outliers and impulsive noises) are not uncommon in practice. The usual minimum mean-square error (MMSE) criterion, which can be easily achieved with KF algorithms, would be largely violated due to the non-Gaussian noises. In this case, a natural idea is to seek more appropriate criteria for filtering problems under the non-Gaussianity constraints. In this regard, the maximum correntropy criterion (MCC) has been proposed in the literature with promising applications to robust adaptive filtering problems in impulsively noisy environments [4]. In particular, the maximum-correntropy-based Kalman filtering (MCKF) problem has recently received some initial research attention and elegant results have begun to appear [14]. For example, in [2] and [3], the MCKF scheme has been verified to perform very well against non-Gaussian noises.

In system modeling, parameter uncertainties are inevitable for a variety of reasons such as modeling errors, exceptional environment disturbance, varying geometry and material properties, change of system load, random failures and repairs of system components [38]. Note that, the occurrence of parameter uncertainties often exhibits a random nature due primarily to the unpredictable changes, and this gives rise to the so-called randomly occurring uncertainties (ROUs) that are typically governed by Bernoulli distributed stochastic variables [32]. The phenomenon of ROUs, if not dedicatedly tackled, would impair the global optimality of the state estimation problems [9], [36], thereby leading to undesirable deterioration of estimation performance. An alternative solution to the ROU-induced problem is to achieve an acceptable bound (rather than the minimum bound) on the performance index and, in this regard, a few Gaussianity-based state estimation strategies have been developed under the MMSE criterion, see e.g. [39]. Nevertheless, the corresponding MCKF problem has not been fully investigated yet for the non-Gaussian systems with ROUs, and this constitutes the main motivation of our current investigation.

The past few decades have seen an ever-lasting enthusiasm towards the research on networked systems (NSs) for their outstanding capability in remote operation and resource sharing. In an ideal situation, the data transmission between all system components (e.g. sensors, controllers, filters and actuators) is implemented via shared communication networks [37]. Compared to traditional point-to-point systems, NSs are more susceptible to the inherent characteristics of networks such as limited network bandwidth and resource constraints. Noting that simultaneous data interactions between multiple components are likely to result in data collisions and subsequently system performance deterioration. As such, it is of vital importance to utilize certain protocols/mechanisms to orchestrate data transmission with aim to reduce unnecessary data exchange in NSs. Accordingly, special attention has been devoted to the analysis/synthesis problems for NSs under communication protocols/mechanisms such as Round-Robin protocol, Try-Once-Discard protocol, stochastic communication protocol and event-triggered mechanism (ETM) [5], [27],

[29], [35], [41].

Among various communication protocols/mechanisms, the ETM has recently become a rather hot topic owing to its attractive advantage in improving utilization efficiency of communication resources [7], [23], [33]. Specifically, the communication resource under an ETM will be occupied only when a certain triggering event happens, and therefore the unnecessarily frequent data exchanges will be avoided, thereby leading to considerable reduction of the network burden. In the past few years, a great many results have been reported on the applications of the ETM in a variety of state estimation problems [30], [40], [42], [43]. For example, the remote state estimation problem has been investigated in [10] for a class of Gaussian systems under the energy-dependent ETM and the MMSE estimate of the energy level has been provided. In [12], a state estimator has been developed for stochastic hybrid systems subject to both ETM and missing measurements. Despite the rich literature on ETM-based state estimation problems, the MCKF problem under ETMs has not been adequately examined and the main purpose of this paper is therefore to bridge such a gap.

Motivated by the above discussions, the main objective of this paper is to design an MCKF scheme for a class of linear time-varying systems under joint effects of the non-Gaussian noises, the ROUs and the event-triggered mechanism. This problem appears to be especially difficult as we are facing three essential challenges as follows: 1) how to construct a reasonable performance index for the Kalman filter design problem within a non-Gaussian environment? 2) how to derive the filter gain in a recursive manner based on the MCC? and 3) how to properly compensate for the joint effects from the ROUs, the non-Gaussian noises and the ETM on the design and performance analysis of the filter? In the current study, we strive to overcome above-mentioned challenges.

The main contributions of this paper are highlighted as follows: *1) the event-based MCKF problem is, for the first time, investigated for the linear time-varying non-Gaussian systems with the ROUs; 2) a novel performance index is proposed to account for the joint effects from the non-Gaussian noises, the ROUs and the ETM; and 3) an MCKF algorithm is developed for the linear time-varying non-Gaussian system where the filter gain is obtained by maximizing the performance index via the matrix analysis approach.* The rest of this paper is organized as follows. In Section II, the MCKF problem under consideration is mathematically formulated. The main results are presented in Section III where the MCKF algorithm is designed by considering the ETM and the ROUs. Section IV demonstrates the effectiveness of the developed MCKF algorithm via a target tracking example. Finally, this paper is concluded in Section V.

Notation. The notation used in this paper is fairly standard except where otherwise stated. $\mathbb{R}^n$ denotes the n-dimensional Euclidean space. $\mathbb{N}^+$ is the set of positive integers. $\Pr\{X\}$ denotes the occurrence probability of a discrete event X. $\mathbb{E}\{\alpha\}$ represents the expectation of a stochastic variable α. $N(u, \Sigma)$ represents the Gaussian probability density function with mean u and covariance Σ. Given a positive definite matrix $M \in \mathbb{R}^{n\times n}$ and a real-valued vector $\beta \in \mathbb{R}^n$, the notations $\|\beta\|$ and $\|\beta\|_M \triangleq \left(\beta^T M\beta\right)^{1/2}$ stand for, respectively, the Euclidean norm and the weighted norm of β. For a matrix A, A^T, A^{-1} and tr(A) represent, respectively, the transpose, inverse and trace of the matrix A, and $A > 0$ means that the matrix A is positive definite. $\mathrm{diag}([a_1, a_2, \ldots, a_n])$ represents a diagonal matrix with elements $a_1, a_2, \ldots, a_n$ on the diagonal. n-dimensional identity matrix is denoted simply as I, and **0** stands for the zero matrix of appropriate dimensions.

II. Problem Formulation

Consider the following class of discrete linear time-varying system

$$\begin{cases} x_{k+1} = (A_k + \alpha_k \Delta A_k)x_k + w_k \\ y_k = C_k x_k + v_k \end{cases} \tag{1}$$

where $x_k \in \mathbb{R}^{n_x}$ and $y_k \in \mathbb{R}^{n_y}$ are, respectively, the system state vector and the measurement output at the time step k; A_k and C_k are real-valued time-varying but known matrices of appropriate dimensions; $w_k \in \mathbb{R}^{n_x}$ and $v_k \in \mathbb{R}^{n_y}$ stand for, respectively, the process noise and measurement noise, which are non-Gaussian variables with covariances $Q_k > 0$ and $R_k > 0$. The initial state x_0 is a stochastic variable with mean $\bar{x}_0$ and covariance P_0.

In the system model (1), ΔA_k is a time-varying real-valued matrix representing norm-bounded parameter uncertainties with the following structure

$$\Delta A_k = M_k U_k N_k \tag{2}$$

where M_k and N_k are known matrices of appropriate dimensions, U_k is an unknown matrix function that describes the time-varying uncertainties with the constraint

$$U_k U_k^T \leq I. \tag{3}$$

In order to characterize the random occurrence of the parameter uncertainties, a Bernoulli-distributed stochastic variable α_k (taking values on 0 or 1) is employed with the probabilities

$$\begin{cases} \Pr\{\alpha_k = 1\} = \bar{\alpha} \\ \Pr\{\alpha_k = 0\} = 1 - \bar{\alpha} \end{cases} \tag{4}$$

where $\bar{\alpha} \in [0, 1]$ is a known scalar that delivers the occurrence probability of the parameter uncertainties. Without loss of generality, in this paper, the process noise w_k, the measurement noise v_k, the stochastic variable α_k and the initial state x_0 are assumed to be mutually independent.

A. *The Event-Triggered Mechanism*

In order to avert frequent data transmission and reduce the consumption of communication resources, the ETM is introduced in the sensor-to-filter channel to schedule the measurement transmission.

Define the triggering time sequence $\mathbb{T} \triangleq \{t_1, t_2, \ldots, t_s, \ldots\}$ with $0 < t_1 < t_2 < \ldots < t_s < \ldots$, which is determined iteratively based on the following triggering condition

$$t_{s+1} = \min\left\{k \in \mathbb{N}^+ | k > t_s, f(e_k, \delta) > 0\right\} \tag{5}$$

where $e_k \triangleq y_{t_s} - y_k$ reflects the change between the current measurement output y_k and the latest transmitted measurement y_{t_s}, and δ is a predefined threshold. Moreover, the event generator function $f(\cdot,\cdot) : \mathbb{R}^{n_y} \times \mathbb{R} \mapsto \mathbb{R}$ is defined as

$$f(e_k, \delta) = e_k^T e_k - \delta \tag{6}$$

and the measurement transmissions will occur only when the condition $f(e_k, \delta) > 0$ is fulfilled.

Under the ETM defined above and the zero-order holder (adopted to maintain the last transmitted measurement signal before the next triggering instant), the actual filter input at the instant k is denoted as

$$\bar{y}_k = y_{t_s}, \forall k \in [t_s, t_{s+1}). \tag{7}$$

B. Maximum-Correntropy-Based Kalman Filter

As is well known, the Kalman filter is considered as an optimal estimator for the linear systems with Gaussian noises under the MMSE criterion. In this context, the minimum trace of the estimation error covariance can be achieved by designing a suitable filter gain. Unfortunately, it is often the case in practice that the systems are subject to the non-Gaussian noises such as impulse noise and unexpected outliers. Statically, the *higher-order moments* of non-Gaussian distributions are crucially important and should be adequately reflected in the corresponding filter design. Inspired by this idea, the so-called correntropy has been introduced as an effective design criterion in [20], which is effectively a localized similarity measure between two scalar stochastic variables:

$$V\left(X,Y\right)=\mathbb{E}\left\{\kappa\left(X,Y\right)\right\}=\int\int\kappa\left(x,y\right)f_{XY}\left(x,y\right)dxdy \tag{8}$$

where $V(X,Y)$ is the correntropy between the stochastic variables X and Y, $f_{XY}(x,y)$ is the joint density function, and $\kappa(\cdot,\cdot)$ is a shift-invariant Mercer kernel function.

Without loss of generality, the Gaussian kernel is used in this paper as the kernel function, which is expressed as

$$\kappa\left(x,y\right)\triangleq G_{\gamma}(\epsilon)=\exp(-\frac{\|\epsilon\|^2}{2\gamma^2}) \tag{9}$$

where $\epsilon\triangleq x-y$ reflects the difference between variables x and y, and γ is a hyper-parameter related to the bandwidth of the kernel size. In addition, due to the fact that the analytical expression of $f_{XY}(x,y)$ is usually unknown, we have to draw samples from $f_{XY}(x,y)$ to estimate (8), i.e.

$$V(X,Y)\approx\frac{1}{N}\sum_{i=1}^{N}\exp(-\frac{\|\epsilon_i\|^2}{2\gamma^2}) \tag{10}$$

where $\epsilon_i\triangleq x_i-y_i$ and $\{x_i,y_i\}_{i=1}^N$ represents the N samples drawn from $f_{XY}(x,y)$.

Remark 1: With the expression given in (9), the correntropy would reach its maximum if and only if $x=y$. Furthermore, as discussed in [2], the correntropy is found to be a weighted sum of all the even-order moments of the difference between the two stochastic variables. By considering the influence of the higher-order moments, the so-called MCC plays a surprisingly effective role in dealing with non-Gaussian noises (e.g. impulse noises or undesirable outliers). Note that the hyper-parameter γ will also affect the estimation performance since the value of γ provides a trade-off between the second- and higher-order moments the correntropy. When $\gamma\to\infty$, the correntropy will be dominated by the second-order moment. The selection of the parameter γ should be in accordance with the noise distribution.

In this paper, to estimate the state of linear time-varying system (1), we construct the Kalman filter as follows:

$$\begin{cases}\hat{x}_{k|k-1}=&A_{k-1}\hat{x}_{k-1|k-1}\\ \hat{x}_{k|k}=&\hat{x}_{k|k-1}+K_k^*(\bar{y}_k-C_k\hat{x}_{k|k-1})\end{cases} \tag{11}$$

where $\hat{x}_{k|k-1}$ and $\hat{x}_{k|k}$ are, respectively, the one-step prediction and corrected state estimate at the time step k. K_k^* is the filter gain that needs to be designed.

To facilitate the subsequent presentation, we denote

$$\tilde{x}_{k|k-1}\triangleq x_k-\hat{x}_{k|k-1},\quad P_{k|k-1}\triangleq\mathbb{E}\{\tilde{x}_{k|k-1}\tilde{x}_{k|k-1}^T\},\quad \tilde{x}_{k|k}\triangleq x_k-\hat{x}_{k|k},\quad P_{k|k}\triangleq\mathbb{E}\{\tilde{x}_{k|k}\tilde{x}_{k|k}^T\}$$

where $\tilde{x}_{k|k-1}$ and $P_{k|k-1}$ stand for the one-step prediction error and its covariance, while $\tilde{x}_{k|k}$ and $P_{k|k}$ are the estimation error and the corresponding covariance at the time step k respectively.

Considering the influence of the non-Gaussian noises, the MCC is employed to formulate the performance index for the proposed filter. Inspired by the work in [11], two objectives are actually embedded into the performance index for the filter design, where the weighting matrices contribute to the minimum-variance estimation, and a maximized correntropy helps to better utilize the higher-order moments of the estimation error distribution. Therefore, we are now able to propose the following correntropy-based performance index:

$$\mathcal{J}_{\mathcal{C}} = \kappa(\bar{y}_k, C_k\hat{x}_{k|k}) + \kappa(\hat{x}_{k|k}, \hat{x}_{k|k-1}) = G_\gamma\left(\left\|\bar{y}_k - C_k\hat{x}_{k|k}\right\|_{R_k^{-1}}\right) + G_\gamma\left(\left\|\hat{x}_{k|k} - \hat{x}_{k|k-1}\right\|_{\Xi_{k|k-1}^{-1}}\right) \tag{12}$$

where $\Xi_{k|k-1}$ is the weighted matrix used to adjust the effects of the one-step prediction error. It can be found from (12) that the correntropy-based performance index $\mathcal{J}_{\mathcal{C}}$ is consisted of two parts, where the first one reflects the estimation performance associated with the "correction", and the second part describes the estimation performance associated with the "prediction". The matrices R_k and $\Xi_{k|k-1}$ are utilized to account for the weights of "correction part" and "prediction part". Compared with the standard correntropy-based performance index, the novelty of our proposed performance index lies in the capability of dealing with the effects induced by the ETM and ROUs. The desired state estimate is achieved by solving the following optimization problem

$$\hat{x}_{k|k} = \arg\max \mathcal{J}_{\mathcal{C}}. \tag{13}$$

Remark 2: In contrast with the conventional Kalman filter which can only guarantee optimality under the Gaussian noise assumption and the MMSE criterion, two noteworthy advantages of the proposed filter (11) can be encapsulated as follows: 1) the non-Gaussian noises can be processed by the filter (11), which is based on the MCC; 2) different from some existing works [13], [14], [31], the filter (11) provides an effective solution to the filtering problem with simultaneous existence of the ETM and the ROUs. It is worth mentioning that the filter (11) is quite similar to the conventional Kalman filter. The main difference between our developed filtering method and the conventional Kalman filtering approach lies in the performance index given in (12). More specifically, the state estimate of the conventional Kalman filtering scheme is derived by **minimizing** the trace of the filtering error covariance, while the state estimate of our proposed maximum-correntropy-based Kalman filtering is achieved by solving the **maximization problem** (13).

Remark 3: In this paper, the ETM is adopted to determine whether the current measurement output should be transmitted to the filter with the hope to reduce the communication load. Obviously, the utilization of the ETM would lead to certain ETM-induced error (i.e. e_k) in the filtering process and thereby affecting the filtering result. Hence, a special correntropy-based performance index (12) is constructed to account for such ETM-induced error by using the upper bound of the one-step prediction error covariance $\Xi_{k|k-1}$.

In summary, due to the induced error from the ROUs and ETM, it would be intractable to parameterize the exact correntropy dynamics with an analytical expression. As an alternative solution, the newly proposed performance index $\mathcal{J}_{\mathcal{C}}$ is used for the filter design in this paper, where the main objective is to first derive an explicit form of the proposed performance index, and then develop an MCKF algorithm to attenuate the effects from the ROUs and ETM on the estimation performance.

III. Main Results

In this section, the upper bound of the one-step prediction error covariance is obtained and the estimation error covariance is derived to further clarify the expression of $\mathcal{J}_{\mathcal{C}}$. Afterwards, an explicit form of the filter gain is also given by maximizing the performance index at each time step.

According to (1) and (11), the dynamics of the one-step prediction error and estimation error can be expressed as

$$\begin{aligned}\tilde{x}_{k|k-1} =&(A_{k-1}+\alpha_{k-1}\Delta A_{k-1})x_{k-1}+w_{k-1}-A_{k-1}\hat{x}_{k-1|k-1}\\ =&A_{k-1}\tilde{x}_{k-1|k-1}+\alpha_{k-1}\Delta A_{k-1}x_{k-1}+w_{k-1}\end{aligned} \tag{14}$$

and

$$\begin{aligned}\tilde{x}_{k|k} =&x_k-\left(\hat{x}_{k|k-1}+K_k^*(\bar{y}_k-C_k\hat{x}_{k|k-1})\right)\\ =&\tilde{x}_{k|k-1}-K_k^*\left(C_k\tilde{x}_{k|k-1}+e_k+v_k\right)\\ =&\left(I-K_k^*C_k\right)\tilde{x}_{k|k-1}-K_k^*e_k-K_k^*v_k.\end{aligned} \tag{15}$$

Consequently, the one-step prediction error covariance and the estimation error covariance can be computed in a recursive form. It follows from (14) that

$$\begin{aligned}P_{k|k-1} =&\mathbb{E}\Big\{\left(A_{k-1}\tilde{x}_{k-1|k-1}+\alpha_{k-1}\Delta A_{k-1}x_{k-1}+w_{k-1}\right)\left(A_{k-1}\tilde{x}_{k-1|k-1}+\alpha_{k-1}\Delta A_{k-1}x_{k-1}+w_{k-1}\right)^T\Big\}\\ =&A_{k-1}P_{k-1|k-1}A_{k-1}^T+\bar{\alpha}\Delta A_{k-1}\mathbb{E}\{x_{k-1}x_{k-1}^T\}\Delta A_{k-1}^T+\mathscr{L}_{k-1}+\mathscr{L}_{k-1}^T+\mathscr{M}_{k-1}+\mathscr{M}_{k-1}^T\\ &+\mathscr{N}_{k-1}+\mathscr{N}_{k-1}^T+Q_{k-1}\end{aligned} \tag{16}$$

where

$$\begin{aligned}&\mathscr{L}_{k-1}\triangleq\bar{\alpha}A_{k-1}\mathbb{E}\left\{\tilde{x}_{k-1|k-1}x_{k-1}^T\right\}\Delta A_{k-1}^T,\quad \mathscr{M}_{k-1}\triangleq A_{k-1}\mathbb{E}\left\{\tilde{x}_{k-1|k-1}w_{k-1}^T\right\}\\ &\mathscr{N}_{k-1}\triangleq\bar{\alpha}\Delta A_{k-1}\mathbb{E}\left\{x_{k-1}w_{k-1}^T\right\}.\end{aligned}$$

Since the process noise w_{k-1} is independent of both $\tilde{x}_{k-1|k-1}$ and x_{k-1}, it is quite straightforward to see that the terms $\mathscr{M}_{k-1}$ and $\mathscr{N}_{k-1}$ are both zero. However, the expectation of another cross term $\mathbb{E}\left\{\tilde{x}_{k-1|k-1}x_{k-1}^T\right\}$ is obviously non-zero, which deserves special attention here and a simplified expression for $P_{k|k-1}$ is then given as

$$P_{k|k-1}=A_{k-1}P_{k-1|k-1}A_{k-1}^T+\mathscr{L}_{k-1}+\mathscr{L}_{k-1}^T+Q_{k-1}+\bar{\alpha}\Delta A_{k-1}\mathbb{E}\{x_{k-1}x_{k-1}^T\}\Delta A_{k-1}^T. \tag{17}$$

Similarly, the recursion of the estimation error covariance is obtained as follows

$$\begin{aligned}P_{k|k} =&\mathbb{E}\Big\{\left(\left(I-K_k^*C_k\right)\tilde{x}_{k|k-1}-K_k^*e_k-K_k^*v_k\right)\left(\left(I-K_k^*C_k\right)\tilde{x}_{k|k-1}-K_k^*e_k-K_k^*v_k\right)^T\Big\}\\ =&\left(I-K_k^*C_k\right)P_{k|k-1}\left(I-K_k^*C_k\right)^T+K_k^*\mathbb{E}\left\{e_ke_k^T\right\}\left(K_k^*\right)^T+K_k^*R_k\left(K_k^*\right)^T\\ &-\mathscr{Q}_k-\mathscr{Q}_k^T+\mathscr{R}_k+\mathscr{R}_k^T-\mathscr{S}_k-\mathscr{S}_k^T\end{aligned} \tag{18}$$

where

$$\begin{aligned}&\mathscr{Q}_k\triangleq\left(I-K_k^*C_k\right)\mathbb{E}\left\{\tilde{x}_{k|k-1}e_k^T\right\}\left(K_k^*\right)^T,\quad \mathscr{R}_k\triangleq K_k^*\mathbb{E}\left\{e_kv_k^T\right\}\left(K_k^*\right)^T,\\ &\mathscr{S}_k\triangleq\left(I-K_k^*C_k\right)\mathbb{E}\left\{\tilde{x}_{k|k-1}v_k^T\right\}\left(K_k^*\right)^T.\end{aligned}$$

Among the above three cross terms, $\mathscr{S}_k$ is zero since the measurement noise is independent of the prediction error. Therefore, the estimation error covariance $P_{k|k}$ is further simplified as

$$\begin{aligned} P_{k|k} = & \left(I - K_k^* C_k\right) P_{k|k-1} \left(I - K_k^* C_k\right)^T + K_k^* R_k \left(K_k^*\right)^T + K_k^* \mathbb{E}\left\{e_k e_k^T\right\} \left(K_k^*\right)^T \\ & - \mathscr{Q}_k - \mathscr{Q}_k^T + \mathscr{R}_k + \mathscr{R}_k^T. \end{aligned} \tag{19}$$

Remark 4: It should be pointed out that the maximum-correntropy-based Kalman filtering has already been studied in the literature. In a standard maximum-correntropy-based Kalman filtering, the correntropy-based performance index is constructed based on the one-step prediction error covariance. Due to the co-existence of the ROUs and the ETM, some terms in the one-step prediction error covariance matrix $P_{k|k-1}$ become unknown, and this further enhances the impossibility of computing the exact value of $P_{k|k-1}$. As such, the general weighted correntropy-based performance index is not applicable to the problem addressed in this paper. To get over such a difficulty, we take the initiative to search for an upper bound of the one-step prediction error covariance and apply the obtained upper bound in the expression of performance index $\mathcal{J}_\mathcal{C}$ (as an alternative performance index). Owing to the fact that the computation procedures of the one-step prediction error covariance and the estimation error covariance are in a coupled and recursive form, the corresponding upper bound of the estimation error covariance is also required.

Lemma 1: For given positive scalars $\beta_i (i = 1, 2, 3, 4)$ and filter gain K_k^*, assume that the following two coupled equations are solvable with the positive definite solutions $\Xi_{k|k-1}$ and $\Xi_{k|k}$:

$$\Xi_{k|k-1} = \left(1 + \bar{\alpha}\beta_1\right) A_{k-1} \Xi_{k-1|k-1} A_{k-1}^T + Q_{k-1} + \left(\bar{\alpha} + \bar{\alpha}\beta_1^{-1}\right) \mathrm{tr}\left\{N_{k-1} \bar{\mathscr{P}}_{k-1} N_{k-1}^T\right\} M_{k-1} M_{k-1}^T \tag{20}$$

and

$$\Xi_{k|k} = \left(1 + \beta_3\right) \left(I - K_k^* C_k\right) \Xi_{k|k-1} \left(I - K_k^* C_k\right)^T + K_k^* \Bigg(\left(1 + \beta_4\right) R_k + \delta \left(1 + \beta_3^{-1} + \beta_4^{-1}\right) I \Bigg) \left(K_k^*\right)^T \tag{21}$$

with the initial condition $\Xi_{0|0} = P_{0|0}$, where

$$\bar{\mathscr{P}}_{k-1} \triangleq \left(1 + \beta_2\right) \Xi_{k-1|k-1} + \left(1 + \beta_2^{-1}\right) \hat{x}_{k-1|k-1} \hat{x}_{k-1|k-1}^T.$$

Then, the one-step prediction error covariance $P_{k|k-1}$ and estimation error covariance $P_{k|k}$ in (17) and (19) satisfy

$$P_{k|k-1} \leq \Xi_{k|k-1}, \;\; P_{k|k} \leq \Xi_{k|k}.$$

Proof: To begin with, let us deal with the unknown terms in the expression of $P_{k|k-1}$. In virtue of the elementary inequality ($mn^T + nm^T \leq \beta mm^T + \beta^{-1} nn^T$ where m and n are vectors of compatible dimensions and β is a scalar), we have

$$\mathscr{L}_{k-1} + \mathscr{L}_{k-1}^T \leq \bar{\alpha}\beta_1 A_{k-1} P_{k-1|k-1} A_{k-1}^T + \bar{\alpha}\beta_1^{-1} \Delta A_{k-1} \mathbb{E}\left\{x_{k-1} x_{k-1}^T\right\} \Delta A_{k-1}^T \tag{22}$$

and

$$\mathbb{E}\left\{\tilde{x}_{k-1|k-1} \hat{x}_{k-1|k-1}^T\right\} + \mathbb{E}\left\{\hat{x}_{k-1|k-1} \tilde{x}_{k-1|k-1}^T\right\} \leq \beta_2 P_{k-1|k-1} + \beta_2^{-1} \hat{x}_{k-1|k-1} \hat{x}_{k-1|k-1}^T.$$

On the other hand, it is easily derived that

$$\begin{aligned} \mathbb{E}\left\{x_{k-1} x_{k-1}^T\right\} = & \mathbb{E}\left\{\left(\tilde{x}_{k-1|k-1} + \hat{x}_{k-1|k-1}\right) \left(\tilde{x}_{k-1|k-1} + \hat{x}_{k-1|k-1}\right)^T\right\} \\ \leq & \left(1 + \beta_2\right) P_{k-1|k-1} + \left(1 + \beta_2^{-1}\right) \hat{x}_{k-1|k-1} \hat{x}_{k-1|k-1}^T \triangleq \mathscr{P}_{k-1}. \end{aligned} \tag{23}$$

Together with (2), (3) and (23), we are now in a position to tackle the uncertainty-related term as follows:

$$\begin{aligned} &\Delta A_{k-1}\mathbb{E}\left\{x_{k-1}x_{k-1}^T\right\}\Delta A_{k-1}^T \\ =&M_{k-1}U_{k-1}N_{k-1}\mathbb{E}\left\{x_{k-1}x_{k-1}^T\right\}N_{k-1}^T U_{k-1}^T M_{k-1}^T \\ \leq&M_{k-1}U_{k-1}N_{k-1}\mathscr{P}_{k-1}N_{k-1}^T U_{k-1}^T M_{k-1}^T \\ \leq&\mathrm{tr}\left\{N_{k-1}\mathscr{P}_{k-1}N_{k-1}^T\right\}M_{k-1}M_{k-1}^T. \end{aligned} \tag{24}$$

Thus, based on (17), (22) and (24), we have

$$P_{k|k-1} \leq (1+\bar{\alpha}\beta_1)A_{k-1}P_{k-1|k-1}A_{k-1}^T + Q_{k-1} + \left(\bar{\alpha}+\bar{\alpha}\beta_1^{-1}\right)\mathrm{tr}\left\{N_{k-1}\mathscr{P}_{k-1}N_{k-1}^T\right\}M_{k-1}M_{k-1}^T. \tag{25}$$

According to the ETM, the measurement gap e_k would be automatically reset to zero when the triggering condition (5) is fulfilled, which implies that $e_k^T e_k \leq \delta$ is always satisfied. By means of the properties of matrix operations, it is easy to obtain

$$\mathbb{E}\left\{e_k e_k^T\right\} \leq \mathbb{E}\left\{\|e_k\|^2 I\right\} = \mathbb{E}\left\{e_k^T e_k I\right\} \leq \delta I, \tag{26}$$

and it then follows from $\mathscr{Q}_k$ and $\mathscr{R}_k$ that

$$-\mathscr{Q}_k - \mathscr{Q}_k^T \leq \beta_3\left(I-K_k^*C_k\right)P_{k|k-1}\left(I-K_k^*C_k\right)^T + \delta\beta_3^{-1}K_k^*\left(K_k^*\right)^T \tag{27}$$

$$\mathscr{R}_k + \mathscr{R}_k^T \leq \beta_4 K_k^* R_k\left(K_k^*\right)^T + \delta\beta_4^{-1}K_k^*\left(K_k^*\right)^T. \tag{28}$$

Thus, according to (19), (27) and (28), we have the following inequality:

$$P_{k|k} \leq (1+\beta_3)\left(I-K_k^*C_k\right)P_{k|k-1}\left(I-K_k^*C_k\right)^T + K_k^*\left((1+\beta_4)R_k + \delta\left(1+\beta_3^{-1}+\beta_4^{-1}\right)I\right)\left(K_k^*\right)^T. \tag{29}$$

Next, in virtue of the mathematical induction approach, the upper bound of the one-step prediction error covariance and the estimation error covariance can be determined as

$$P_{k|k-1} \leq \Xi_{k|k-1},\ \ P_{k|k} \leq \Xi_{k|k},$$

which completes the proof. ■

Based on the performance index $\mathcal{J}_{\mathcal{C}}$ given in (12), we are now ready to obtain the state estimate by finding a feasible solution for the following optimization problem

$$\hat{x}_{k|k} = \arg\max \mathcal{J}_{\mathcal{C}} \tag{30}$$

Taking the partial derivative of $\mathcal{J}_{\mathcal{C}}$ with respect to $\hat{x}_{k|k}$, we have

$$\begin{aligned} \frac{\partial \mathcal{J}_{\mathcal{C}}}{\partial \hat{x}_{k|k}} =& -\frac{1}{\gamma^2}G_\gamma\left(\left\|\bar{y}_k - C_k\hat{x}_{k|k}\right\|_{R_k^{-1}}\right)C_k^T R_k^{-1}\left(\bar{y}_k - C_k\hat{x}_{k|k}\right) \\ &+ \frac{1}{\gamma^2}G_\gamma\left(\left\|\hat{x}_{k|k}-\hat{x}_{k|k-1}\right\|_{\Xi_{k|k-1}^{-1}}\right)\Xi_{k|k-1}^{-1}\left(\hat{x}_{k|k}-\hat{x}_{k|k-1}\right). \end{aligned} \tag{31}$$

By letting $\frac{\partial \mathcal{J}_{\mathcal{C}}}{\partial \hat{x}_{k|k}} = 0$, we have

$$\left(\Xi_{k|k-1}^{-1} + L_k C_k^T R_k^{-1} C_k\right)\hat{x}_{k|k} = \Xi_{k|k-1}^{-1}\hat{x}_{k|k-1} + L_k C_k^T R_k^{-1}\bar{y}_k \tag{32}$$

with the auxiliary gain defined as

$$L_k = \frac{G_\gamma\left(\left\|\bar{y}_k - C_k\hat{x}_{k|k}\right\|_{R_k^{-1}}\right)}{G_\gamma\left(\left\|\hat{x}_{k|k} - \hat{x}_{k|k-1}\right\|_{\Xi_{k|k-1}^{-1}}\right)}. \tag{33}$$

Since the item $\hat{x}_{k|k}$ is not available when computing L_k, it becomes impossible to obtain the exact value of the auxiliary gain. Following the widely adopted approximation method in Gaussian-kernel-based entropy filters [11], $\hat{x}_{k|k}$ is substituted by $\hat{x}_{k|k-1}$ for the calculation of L_k in this work. Thus, the denominator in (33) is equal to 1, and the new auxiliary gain represented by L_k^a is given as

$$L_k^a = G_\gamma\left(\left\|\bar{y}_k - C_k\hat{x}_{k|k-1}\right\|_{R_k^{-1}}\right). \tag{34}$$

To derive a recursive expression for the state estimate, (32) is reformulated as

$$\begin{aligned}
&\left(\Xi_{k|k-1}^{-1} + L_k^a C_k^T R_k^{-1} C_k\right)\hat{x}_{k|k} \\
=&\,\Xi_{k|k-1}^{-1}\hat{x}_{k|k-1} + L_k^a C_k^T R_k^{-1} C_k \hat{x}_{k|k-1} + L_k^a C_k^T R_k^{-1}\bar{y}_k - L_k^a C_k^T R_k^{-1} C_k \hat{x}_{k|k-1} \\
=&\left(\Xi_{k|k-1}^{-1} + L_k^a C_k^T R_k^{-1} C_k\right)\hat{x}_{k|k-1} + L_k^a C_k^T R_k^{-1}\left(\bar{y}_k - C_k\hat{x}_{k|k-1}\right),
\end{aligned} \tag{35}$$

and we finally obtain

$$\hat{x}_{k|k} =\hat{x}_{k|k-1} + \left(\Xi_{k|k-1}^{-1} + L_k^a C_k^T R_k^{-1} C_k\right)^{-1} L_k^a C_k^T R_k^{-1}\left(\bar{y}_k - C_k\hat{x}_{k|k-1}\right). \tag{36}$$

Recalling the filter structure given in (11), it is straightforward to acquire the desired filter gain of the following form

$$K_k^* = \left(\Xi_{k|k-1}^{-1} + L_k^a C_k^T R_k^{-1} C_k\right)^{-1} L_k^a C_k^T R_k^{-1} \tag{37}$$

To facilitate the readers to understand the proposed MCKF algorithm with ROUs under ETM, the summarized process is listed in Algorithm 1.

Remark 5: Up to now, we have addressed the MCKF problem for a class of linear time-varying systems with ROUs in non-Gaussian environment, where the data transmissions are governed via the predefined triggering condition. To be more specific, a new correntropy-based performance index has been designed where the effects of the ROUs and the ETM are fully considered, based on which an MCKF algorithm has been designed and the explicit form of the filter gain has been obtained accordingly. It is worth mentioning that the proposed filter is suitable for online state estimation due to the recursive nature of the developed algorithm.

Remark 6: The MCKF problem has stirred much attention due mainly to the prevalence of the non-Gaussian noises and a number of excellent results have been reported in the literature, see e.g. [2], [3]. Compared to existing literature, the main results developed in this paper exhibit the following distinctive features: 1) the proposed MCKF algorithm is capable of resisting the ROUs under a particularly effective ETM; 2) the proposed performance index takes the non-Gaussian noises, the ROUs and the ETM into simultaneous account; and 3) the MCKF algorithm is locally optimal in that the performance index is maximized at each time instant.

Remark 7: One of the main advantages of our proposed MCKF scheme is the capability to deal with the non-Gaussian noises (e.g. impulse noise and unexpected outliers). For such non-Gaussian noises, the

Algorithm 1 MCKF algorithm with ROUs under ETM

Step 1. Parameter initialization

Initialize the vector $\hat{x}_{0|0} = x_0$ and matrix $\Xi_{0|0} = P_0$. Set the maximum recursive time step to be K.

Step 2. One-step prediction

Calculate the one-step prediction according to

$$\hat{x}_{k|k-1} = A_{k-1}\hat{x}_{k-1|k-1}$$

and the upper bound of the one-step prediction error covariance with (20).

Step 3. Estimate correction

Calculate auxiliary gain L_k via (34) and the estimator gain K_k^* with (37). Obtain the corrected estimate as

$$\hat{x}_{k|k} = \hat{x}_{k|k-1} + K_k^*(\bar{y}_k - C_k\hat{x}_{k|k-1}),$$

and compute the upper bound of the estimation error covariance with (21).

Step 4. If $k < K$, then go to Step 2; otherwise go to Step 5.

Step 5. Stop.

higher-order moments of their distributions would lead to significant impact on the measurement data, which makes it difficult to achieve the satisfactory filtering performance by using the traditional Kalman filter. As such, a special correntropy-based performance index is constructed in this work to account for the influence of the higher-order moments. Obviously, based on the filter gain that is computed according to the correntropy-based performance index, our developed MCKF approach is capable of dealing with the effects from non-Gaussian noises.

IV. Illustrative Example

In this section, a simulation example of the target tracking problem is provided to show the validity of the proposed MCKF approach.

A. Target Tracking Scenario

Consider the target tracking problem described by the two-dimensional model with the following matrices:

$$A_k = \begin{bmatrix} 1 & h & 0 & 0 \\ 0 & 1 & 0 & 0 \\ 0 & 0 & 1 & h \\ 0 & 0 & 0 & 1 \end{bmatrix}, \quad C_k = \begin{bmatrix} 1 & 0 & 0 & 0 \\ 0 & 0 & 1 & 0 \end{bmatrix}, \quad M_k = \begin{bmatrix} 0.3 \\ 0.1 \\ 0.2 \\ 0.1 \end{bmatrix}, \quad N_k^T = \begin{bmatrix} 0.1 \\ 0 \\ 0.2 \\ 0.1 \end{bmatrix}, \quad U_k = \sin(3k), \tag{38}$$

where h stands for the sampling period throughout the simulation process, and the state variable at the time step k is defined as $x_k \triangleq \left[\iota_k^{ht},\ \vartheta_k^{ht},\ \iota_k^{vt},\ \vartheta_k^{vt}\right]^T$, where $\left(\iota_k^{ht},\ \iota_k^{vt}\right)$ and $\left(\vartheta_k^{ht},\ \vartheta_k^{vt}\right)$ represent, respectively, the horizontal and vertical coordinates of the target position and velocity. The constant scalar $\bar{\alpha}$ that reflects the occurrence probability of the parameter uncertainties will first take a fixed value, and the effect from this parameter on the estimation performance is to be discussed later in Section IV-D. Both the process

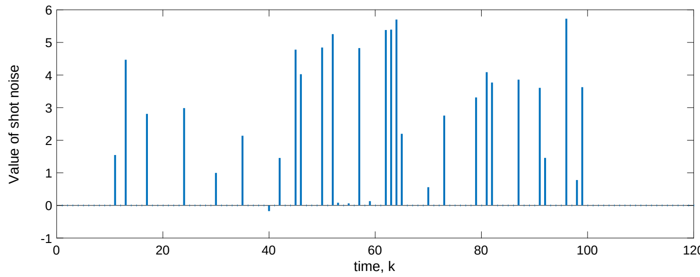

Fig. 1: Shot noise in the process noise

noise and measurement noise are chosen to be non-Gaussian noises. Specifically, the process noise is composed of general Gaussian noise plus shot noise, which is randomly generated with a total number of times n_s during the simulation process of the length T. One example of the shot noise applied to the process noise is given in Fig. 1. The process noise is expressed as

$$w_k = N(\mathbf{0}, \Sigma_w) + \text{shot noise} \tag{39}$$

where the covariance matrix Σ_w is described as

$$\Sigma_w = \sigma_{acc}^2 \begin{bmatrix} \frac{h^3}{3} & \frac{h^2}{2} & 0 & 0 \\ \frac{h^2}{2} & h & 0 & 0 \\ 0 & 0 & \frac{h^3}{3} & \frac{h^2}{2} \\ 0 & 0 & \frac{h^2}{2} & h \end{bmatrix} \tag{40}$$

where σ_{acc}^2 stands for the acceleration variance. Different from the process noise, the measurement noise adopted here is the Gaussian mixture noise with the following form

$$v_k = (1-\bar{p})N(\mathbf{0}, \Sigma_{v_1}) + \bar{p}N(\mathbf{0}, \Sigma_{v_2}) \tag{41}$$

where $\bar{p}$ is the glint probability, and the covariance matrices $\Sigma_{v_i}(i=1,2)$ are both with the form of $\sigma_{v_i}^2 I$.

After obtaining the position information of the target, the sensor utilizes the event generator function (6) to determine whether the triggering condition (5) is fulfilled. If $f(e_k, \delta) > 0$, the sensor will transmit the obtained measurement to the filter, and the corresponding measurement gap e_k will be reset to zero automatically. As the threshold δ increases, the transmission instants are expected to reduce accordingly, and the effect from the threshold value on the estimation performance will be discussed later in Section IV-D as well.

B. Parameter Settings and Performance Metric

During the simulation process, the actual target trajectories are simulated with the initial state $x_0 = [300, 4, 90, 3]^T$. To initialize $\hat{x}_{0|0}$ in the estimation stage, both the position and velocity components are sampled from the respective Gaussian prior distributions. To be more specific, the mean value and covariance matrix for the position components are $[300, 90]^T$ and $\text{diag}([10, 10])$, while a different distribution is utilized for the velocity components with mean $[4, 3]^T$ and covariance matrix $\text{diag}([1, 1])$.

For the evaluation purpose, M independent Monte Carlo trials are conducted to testify the performance of the proposed estimator, and the root mean-square error (RMSE) metric is introduced on both position and velocity estimates averaged over the M trials, which are respectively expressed as

$$\mathrm{RMSE}_{\iota,k} = \sqrt{\frac{1}{M}\sum_{i=1}^{M}\left(\left(\iota_k^{ht,i} - \hat{\iota}_k^{ht,i}\right)^2 + \left(\iota_k^{vt,i} - \hat{\iota}_k^{vt,i}\right)^2\right)}$$

$$\mathrm{RMSE}_{\vartheta,k} = \sqrt{\frac{1}{M}\sum_{i=1}^{M}\left(\left(\vartheta_k^{ht,i} - \hat{\vartheta}_k^{ht,i}\right)^2 + \left(\vartheta_k^{vt,i} - \hat{\vartheta}_k^{vt,i}\right)^2\right)}$$

where $\left(\iota_k^{ht,i}, \iota_k^{vt,i}\right)$ and $\left(\vartheta_k^{ht,i}, \vartheta_k^{vt,i}\right)$ stand for, respectively, the realization of the position and velocity components of the target state within the ith Monte Carlo trial, and $\left(\hat{\iota}_k^{ht,i}, \hat{\iota}_k^{vt,i}\right)$, $\left(\hat{\vartheta}_k^{ht,i}, \hat{\vartheta}_k^{vt,i}\right)$ are their corresponding estimates.

Related parameter settings utilized in the simulation are provided in TABLE I.

TABLE I: Parameter settings

Parameters	Values	Parameters	Values
h	1	T	120
$\bar{\alpha}$	0.7	$\bar{p}$	0.2
n_s	35	σ_{acc}^2	0.1
$\sigma_{v_1}^2$	10	$\sigma_{v_2}^2$	50
δ	30	M	100
β_1	2	β_2	0.5
β_3	0.3	β_4	0.5

C. Results Analysis

For the purpose of comparison, the state estimation will be implemented via the following two filters: 1) the proposed maximum-correntropy-based filter subject to ROUs under the ETM (abbreviated as MC-ET-PU in Figs. 2-5); and 2) the conventional maximum-correntropy-based filter neglecting the influence caused by the ETM and ROUs (abbreviated as MC in Figs. 2-5).

The estimation results obtained by the above two filters for one realization of the target trajectory are shown in Figs. 2-3. It can be seen that the proposed maximum-correntropy-based filter provides a more accurate result and outperforms the conventional maximum-correntropy-based filter with less measurement information and ROUs. The evolution of position RMSEs and velocity RMSEs, calculated based on the estimates from the conventional maximum-correntropy-based filter and the proposed maximum-correntropy-based filter, are shown in Figs. 4-5, respectively. We observe that the proposed maximum-correntropy-based filter provides better performance than that of the conventional maximum-correntropy-based filter, which demonstrates that we have effectively restrained the influences from the ETM and ROUs, and this is due mainly to the fact that we have considered these influences into the design of the estimator.

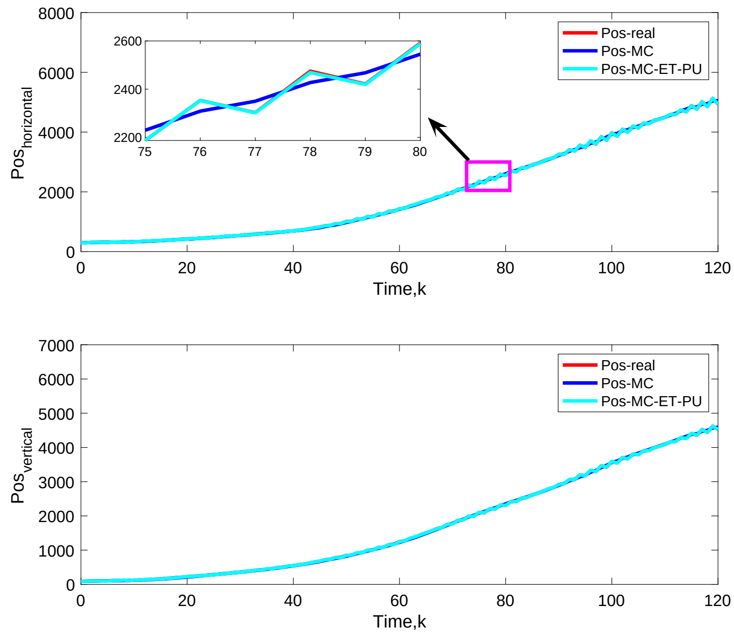

Fig. 2: The position components of the target trajectory and their estimates obtained by MC-ET-PU and MC in one trial.

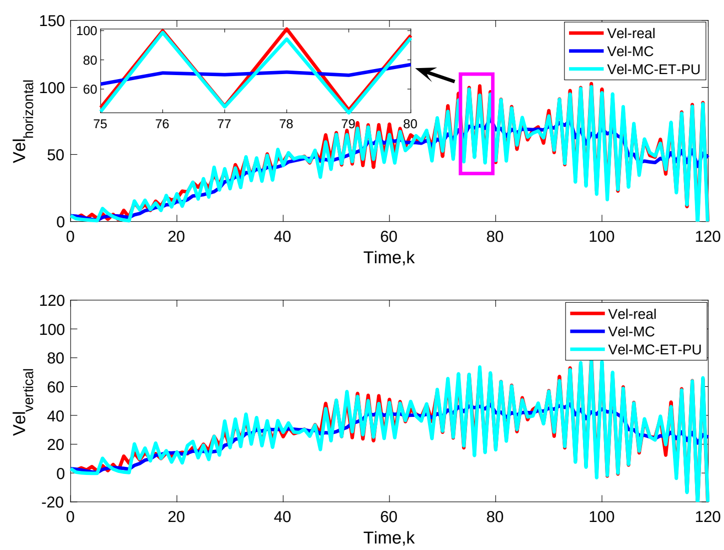

Fig. 3: The velocity components of the target trajectory and their estimates obtained by MC-ET-PU and MC in one trial.

D. Discussion on Parameter Settings

To further investigate the effects from the ROUs and the ETM on the tracking performance, two more groups of simulations are carried out with different parameter settings. In the first group, the only changing parameter is the occurrence probability of parameter uncertainties, and the others remain unchanged. The corresponding behaviors of RMSEs on position and velocity components in the estimation results are

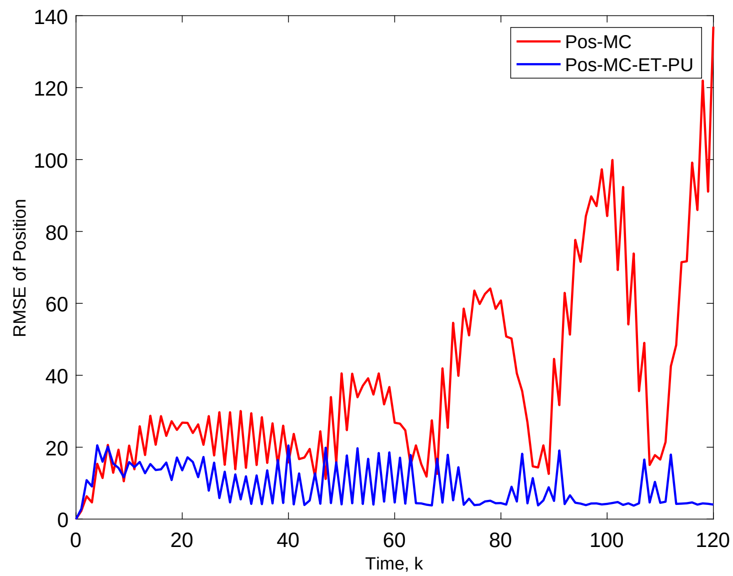

Fig. 4: Position RMSEs of MC-ET-PU and MC.

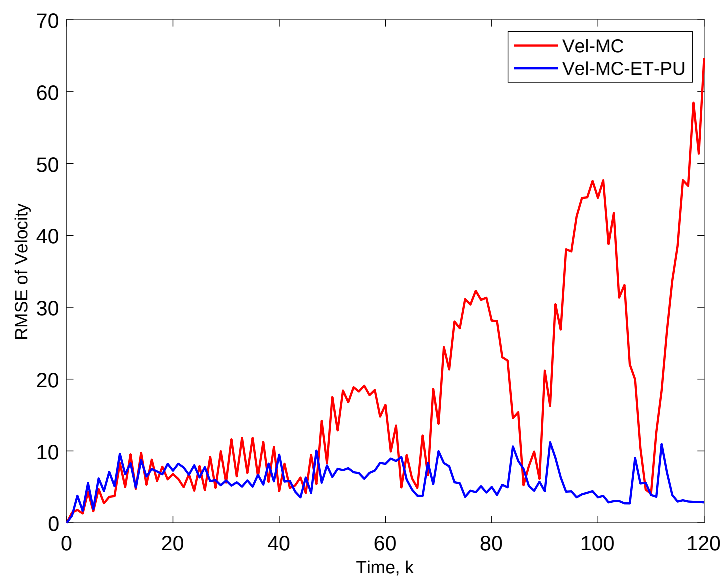

Fig. 5: Velocity RMSEs of MC-ET-PU and MC.

given in Figs. 6-7, where a more obvious impact is found in the comparison of the velocity RMSEs. Since the measurement output is right the position components of the target state, the effect of the randomly occurring uncertainties is not obvious to the position estimates. When it comes to the velocity RMSEs, we observe as expected that the performance clearly degrades as the occurrence probability increases.

Similarly as above, in the second group of simulations, the changing parameter turns into the triggering threshold δ. The related simulation results are given in Figs. 8-9. Due to the fact that a larger threshold leads to much fewer transmissions, the worst performance is found with $\delta = 50$ where the available measurement information at the filter end is significantly reduced. Considering the contradiction between

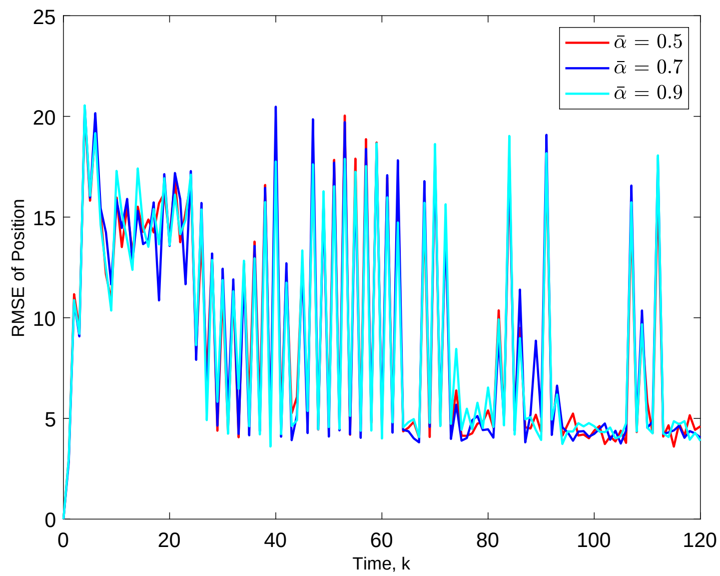

Fig. 6: Position RMSEs of MC-ET-PU with respect to different occurrence probabilities of uncertainties.

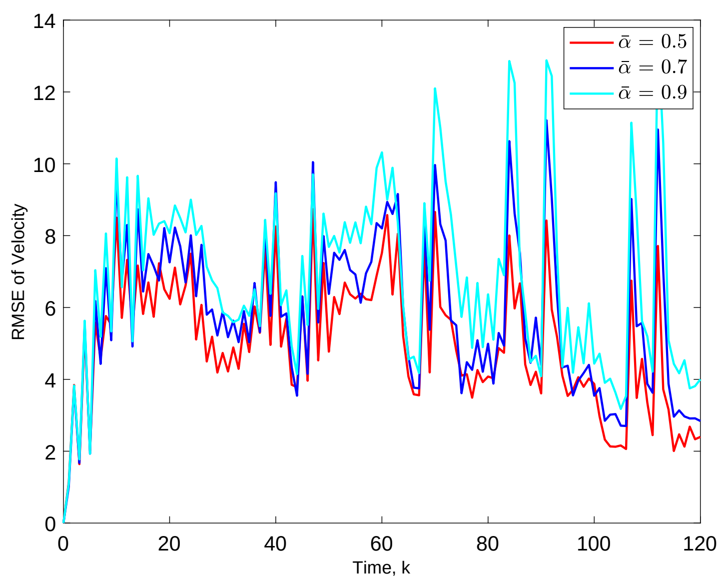

Fig. 7: Velocity RMSEs of MC-ET-PU with respect to different occurrence probabilities of uncertainties.

the communication resource consumption and the estimation performance, a reasonable trade-off is quite necessary, especially in the practical applications.

To demonstrate the effect of the ETM to the communication cost reduction and the estimation performance, the average triggering rate and average RMSEs obtained under different values of threshold are compared in TABLE II. To be more specific, the average triggering rate $\mathfrak{R}$ is calculated as the mean of the triggering rate over all the M Monte Carlo trials. Furthermore, the average RMSEs on position (RMSE_ι^*) and velocity $(\mathrm{RMSE}_\vartheta^*)$ are the mean of $\mathrm{RMSE}_{\iota,k}$ and $\mathrm{RMSE}_{\vartheta,k}$ over the total simulation period. With the increase of the triggering threshold, the average triggering rate decreases obviously, and the estimation

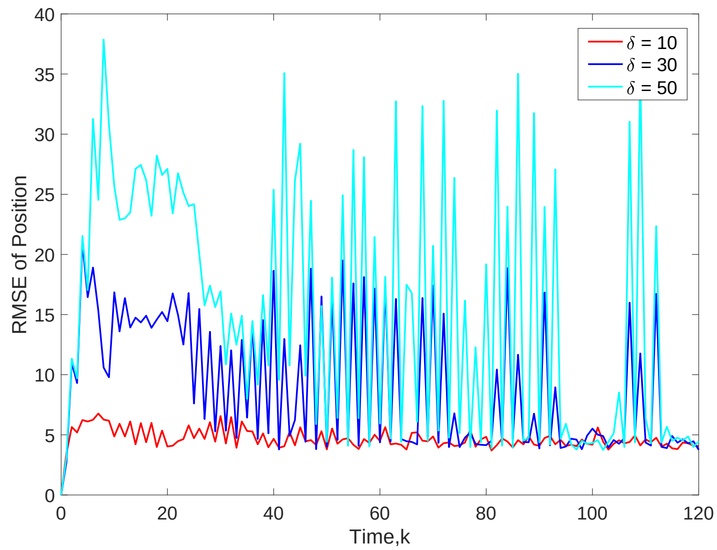

Fig. 8: Position RMSEs of MC-ET-PU with respect to different triggering thresholds.

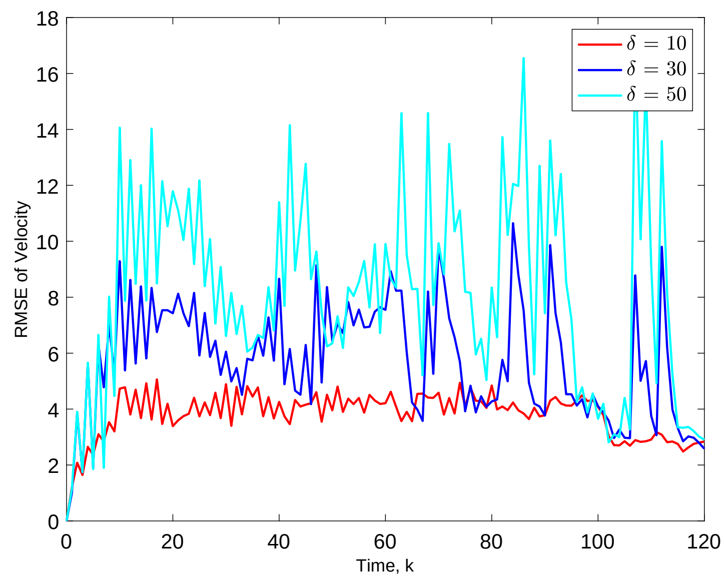

Fig. 9: Velocity RMSEs of MC-ET-PU with respect to different triggering thresholds.

performance also degrades simultaneously.

V. Conclusions

In this paper, the MCKF algorithm has been developed to solve the filtering problem for a class of non-Gaussian systems with the ROUs under ETM. The measurement transmission has been modulated by the ETM and a Bernoulli-distributed stochastic variable has been utilized to regulate the random nature of parameter uncertainties. A performance index has been established, which is suitable for reflecting the joint effects from the non-Gaussian noises, the ETM and the ROUs on the estimation performance. Based on the proposed performance index, an MCKF algorithm has developed, where the MCC has been introduced

TABLE II: The effect of the triggering threshold on the average triggering rate and average RMSEs

	$\mathfrak{R}$	$\mathrm{RMSE}_{\iota}^{*}$	$\mathrm{RMSE}_{\vartheta}^{*}$
$\delta = 10$	90.88%	4.6524	3.8004
$\delta = 30$	70.45%	9.1136	5.7438
$\delta = 50$	58.39%	15.1159	8.1338

to facilitate the calculation of filter gain. Finally, a target tracking example has been provided to illustrate the effectiveness of the proposed MCKF algorithm. Future research topics would include the extension of the correntropy-based criterion to the nonlinear networked systems subject to other communication protocols (e.g. Round-Robin protocol, Try-Once-Discard protocol, Random Access protocol and dynamic event-triggered protocol) [15], [24], [45]–[48] and improvement of the filtering performance by using some latest optimization algorithms [21], [22].

References

[1] I. Arasaratnam and S. Haykin, Cubature Kalman filters, *IEEE Transactions on Automatic Control*, vol. 54, no. 6, pp. 1254–1269, 2009.

[2] B. Chen, X. Liu, H. Zhao and J. C. Principe, Maximum correntropy Kalman filter, *Automatica*, vol. 76, pp. 70–77, 2017.

[3] B. Chen, X. Wang, Y. Li and J. C. Principe, Maximum correntropy criterion with variable center, *IEEE Signal Processing Letters*, vol. 26, no. 8, pp. 1212–1216, 2019.

[4] B. Chen, L. Xing, H. Zhao, N. Zheng and J. C. Principe, Generalized correntropy for robust adaptive filtering, *IEEE Transactions on Signal Processing*, vol. 64, no. 13, pp. 3376–3387, 2016.

[5] Y. Chen, Z. Wang, L. Wang and W. Sheng, Finite-horizon H_∞ state estimation for stochastic coupled networks with random inner couplings using Round-Robin protocol, *IEEE Transactions on Cybernetics*, in press, DOI: 10.1109/TCYB.2020.3004288.

[6] Y. Chen, Z. Wang, L. Wang and W. Sheng, Mixed H_2/H_∞ state estimation for discrete-time switched complex networks with random coupling strengths through redundant channels, *IEEE Transactions on Neural Networks and Learning Systems*, in press, DOI: 10.1109/TNNLS.2019.2952249.

[7] Y. Cui, Y. Liu, W. Zhang and F. E. Alsaadi, Event based consensus for a class of nonlinear multi-agent systems with sequentially connected topology, *IEEE Transactions on Circuits and Systems I: Regular Papers*, vol. 65, no. 10, pp. 3506–3518, Oct. 2018.

[8] N. Hou, Z. Wang, D. W. C. Ho and H. Dong, Robust partial-nodes-based state estimation for complex networks under deception attacks, *IEEE Transactions on Neural Networks and Learning Systems*, vol. 31, no. 6, pp. 2793–2802, Jun. 2020.

[9] J. Hu, Z. Wang, G.-P. Liu and H. Zhang, Variance-constrained recursive state estimation for time-varying complex networks with quantized measurements and uncertain inner coupling, *IEEE Transactions on Neural Networks and Learning Systems*, in press, DOI: 10.1109/TNNLS.2019.2927554.

[10] J. Huang, D. Shi and T. Chen, Event-triggered state estimation with an energy harvesting sensor, *IEEE Transactions on Automatic Control*, vol. 62, no. 9, pp. 4768–4775, 2017.

[11] R. Izanloo, S. Fakoorian, H. Yazdi and D. Simon, Kalman filtering based on the maximum correntropy criterion in the presence of non-Gaussian noise, in *Proceedings of Annual Conference on Information Science and Systems*, Princeton, NJ, USA, 2016, pp. 1–6.

[12] Z. Jin, Y. Hu and C. Sun, Event-triggered state estimation for stochastic hybrid systems with missing measurements, *IET Control Theory & Applications*, vol. 12, no. 18, pp. 2551–2561, 2018.

[13] M. V. Kulikova, Square-root algorithms for maximum correntropy estimation of linear discrete-time systems in presence of non-Gaussian noise, *Systems & Control Letters*, vol. 108, pp. 8–15, 2017.

[14] M. V. Kulikova, Chandrasekhar-based maximum correntropy Kalman filtering with the adaptive kernel size selection, *IEEE Transactions on Automatic Control*, vol. 65, no. 2, pp. 741-748, 2020.

[15] Q. Li, Z. Wang, N. Li and W. Sheng, A dynamic event-triggered approach to recursive filtering for complex networks with switching topologies subject to random sensor failures, *IEEE Transactions on Neural Networks and Learning Systems*, Vol. 31, No. 10, pp. 4381-4388, Oct. 2020.

[16] W. Li, G. Wei, D. Ding, Y. Liu and F. E. Alsaadi, A new look at boundedness of error covariance of Kalman filtering, *IEEE Transactions on Systems, Man, and Cyberneics - Systems*, vol. 48, no. 1, pp. 309–314, 2018.

[17] W. Li, Z. Wang, Q. Liu and L. Guo, An information aware event-triggered scheme for particle filter based remote state estimation, *Automatica*, vol. 103, pp. 151–158, 2019.

[18] Q. Liu and Z. Wang, Moving-horizon estimation for linear dynamic networks with binary encoding schemes, *IEEE Transactions on Automatic Control*, in press, DOI: 10.1109/TAC.2020.2996579.

[19] S. Liu, Z. Wang, G. Wei and M. Li, Distributed set-membership filtering for multi-rate systems under the Round-Robin scheduling over sensor networks, *IEEE Transactions on Cybernetics*, vol. 50, no. 5, pp. 1910–1920, 2020.

[20] W. Liu, P. P. Pokharel and J. C. Principe, Correntropy: Properties and applications in non-Gaussian signal processing, *IEEE Transactions on Signal Processing*, vol. 55, no. 11, pp. 5286–5298, 2007.

[21] Y. Liu, Q. Cheng, Y. Gan, Y. Wang, Z. Li and J. Zhao, Multi-objective optimization of energy consumption in crude oil pipeline transportation system operation based on exergy loss analysis, *Neurocomputing*, vol. 332, pp. 100–110, Mar. 2019.

[22] Y. Liu, S. Chen, B. Guan and P. Xu, Layout optimization of large-scale oil-gas gathering system based on combined optimization strategy, *Neurocomputing*, vol. 332, pp. 159–183, Mar. 2019.

[23] Y. Liu, Z. Wang, Y. Yuan and W. Liu, Event-triggered partial-nodes-based state estimation for delayed complex networks with bounded distributed delays, *IEEE Transactions on Systems, Man, and Cybernetics-Systems*, vol. 49, no. 6, pp. 1088–1098, Jun. 2019.

[24] L. Ma, Z. Wang, C. Cai and F. E. Alsaadi, Dynamic event-triggered state estimation for discrete-time singularly perturbed systems with distributed time-delays, *IEEE Transactions on Systems, Man, and Cybernetics-Systems*, in press, DOI: 10.1109/TSMC.2018.2876203.

[25] B. Qu, N. Li, Y. Liu and F. E. Alsaadi, Estimation for power quality disturbances with multiplicative noises and correlated noises: A recursive estimation approach, *International Journal of Systems Science*, vol. 51, no. 7, pp. 1200–1217, May. 2020.

[26] K. Reif, S. Gunther, E. Yaz and R. Unbehauen, Stochastic stability of the discrete-time extended Kalman filter, *IEEE Transactions on Automatic Control*, vol. 44, no. 4, pp. 714–728, 1999.

[27] B. Shen, Z. Wang, D. Wang and H. Liu, Distributed state-saturated recursive filtering over sensor networks under Round-Robin protocol, *IEEE Transactions on Cybernetics*, vol. 50, no. 8, pp. 3605–3615, Aug. 2020.

[28] Y. Shen, Z. Wang, B. Shen and F. E. Alsaadi, Nonfragile H_∞ filtering for discrete multirate time-delayed systems over sensor networks characterized by Gilbert-Elliott models, *International Journal of Robust and Nonlinear Control*, vol. 30, no. 8, pp. 3194–3214, May. 2020.

[29] Y. Shen, Z. Wang, B. Shen, F. E. Alsaadi and F. E. Alsaadi, Fusion estimation for multi-rate linear repetitive processes under weighted Try-Once-Discard protocol, *Information Fusion*, vol. 55, pp. 281–291, Mar. 2020.

[30] D. Shi, T. Chen and L. Shi, An event-triggered approach to state estimation with multiple point- and set-valued measurements, *Automatica*, vol. 50, no. 6, pp. 1641–1648, 2014.

[31] H. Song, D. Ding, H. Dong, G. Wei and Q.-L. Han, Distributed entropy filtering subject to DoS attacks in non-Gauss environments, *International Journal of Robust and Nonlinear Control*, vol. 30, no. 3, pp. 1240–1257, 2020.

[32] Y. Song, J. Hu, D. Chen, D. Ji and F. Liu, Recursive approach to networked fault estimation with packet dropouts and randomly occurring uncertainties, *Neurocomputing*, vol. 214, pp. 340–349, 2016.

[33] H. Tan, B. Shen, Y. Liu, A. Alsaedi and B. Ahmad, Event-triggered multi-rate fusion estimation for uncertain system with stochastic nonlinearities and colored measurement noises, *Information Fusion*, vol. 36, pp. 313-320, 2017.

[34] H. Tan, B. Shen, K. Peng and H. Liu, Robust recursive filtering for uncertain stochastic systems with amplify-and-forward relays, *International Journal of Systems Science*, vol. 51, no. 7, pp. 1188–1199, May. 2020.

[35] X. Wan, Z. Wang, Q.-L. Han and M. Wu, A recursive approach to quantized H_∞ state estimation for genetic regulatory networks under stochastic communication protocols, *IEEE Transactions on Neural Networks and Learning Systems*, vol. 30, no. 9, pp. 2840–2852, Sept. 2019.

[36] F. Wang, Z. Wang, J. Liang and X. Liu, Resilient state estimation for 2-D time-varying systems with redundant channels: A variance-constrained approach, *IEEE Transactions on Cybernetics*, vol. 49, no. 7, pp. 2479–2489, 2019.

[37] Z. Wang, L. Wang, S. Liu and G. Wei, Encoding-Decoding-Based control and filtering of networked systems: insights, developments and opportunities, *IEEE/CAA Journal of Automatica Sinica*, vol. 5, no. 1, pp. 3–18, 2018.

[38] J. Yang, W. Chen, S. Li, L. Guo and Y. Yan, Disturbance/uncertainty estimation and attenuation techniques in PMSM drives–a survey, *IEEE Transactions on Industrial Electronics*, vol. 64, no. 4, pp. 3273–3285, 2017.

[39] Y. Yang, Y. Liang, L. Xu, Y. Yang and Y. Qin, Upper bound filter under interval constraints and multiplicative noises, *IET Control Theory & Applications*, vol. 13, no. 15, pp. 2482–2491, 2019.

[40] X. Yin and J. Liu, Event-triggered state estimation of linear systems using moving horizon estimation, *IEEE Transactions on Control Systems Technology*, in press, DOI: 10.1109/TCST.2020.2978908.

[41] Y. Yuan, P. Zhang, Z. Wang and Y. Chen, Noncooperative event-triggered control strategy design with Round-Robin protocol:

Applications to load frequency control of circuit systems, *IEEE Transactions on Industrial Electronics*, vol. 67, no. 3, pp. 2155–2166, Mar. 2020.

[42] D. Zhao, Z. Wang, Y. Chen and G. Wei, Proportional-integral observer design for multidelayed sensor-saturated recurrent neural networks: a dynamic event-triggered protocol, *IEEE Transactions on Cybernetics*, Vol. 50, No. 11, pp. 4619-4632, Nov. 2020.

[43] D. Zhao, Z. Wang, G. Wei and Q.-L. Han, A dynamic event-triggered approach to observer-based PID security control subject to deception attacks, *Automatica*, Vol. 120, Art. No. 109128, 13 pages, Oct. 2020.

[44] J. Zhao and L. Mili, A decentralized H_∞ unscented Kalman filter for dynamic state estimation against uncertainties, *IEEE Transactions on Smart Grid*, vol. 10, no. 5, pp. 4870–4880, 2019.

[45] L. Zou, Z. Wang, Q.-L. Han and D. Zhou, Recursive filtering for time-varying systems with random access protocol, *IEEE Transactions on Automatic Control*, vol. 64, no. 2, pp. 720-727, Feb. 2019.

[46] L. Zou, Z. Wang, Q.-L. Han and D. Zhou, Moving horizon estimation for networked time-delay systems under Round-Robin protocol, *IEEE Transactions on Automatic Control*, vol. 64, no. 12, pp. 5191-5198, Dec. 2019.

[47] L. Zou, Z. Wang, Q.-L. Han and D. H. Zhou, Moving horizon estimation of networked nonlinear systems with random access protocol, *IEEE Transactions on Systems, Man, and Cybernetics-Systems*, in press, DOI: 10.1109/TSMC.2019.2918002.

[48] L. Zou, Z. Wang and D. H. Zhou, Moving horizon estimation with non-uniform sampling under component-based dynamic event-triggered transmission, *Automatica*, vol. 120, Art. no. 109154, Oct. 2020.